

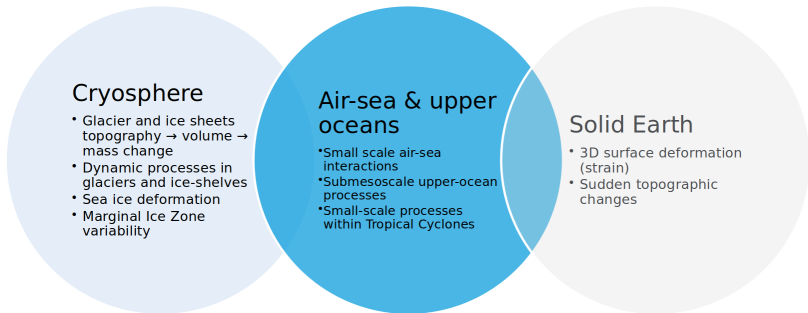
# Harmony's ocean elevation measurements: potential and performance

Andreas Theodosiou, Paco Lopez Dekker, Marcel Kleinherenbrink, Gert Mulder

Delft University of Technology, The Netherlands

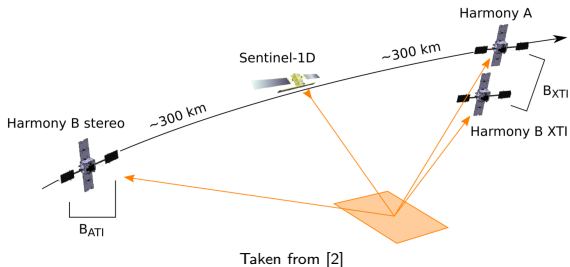
4 May 2020

# Mission Objectives



Adapted from [1]

# Satellite Formations



- Two formations
- Close formation has a cross-track baseline  $\rightarrow$  sensitivity to height
- There is also an along-track baseline  $\rightarrow$  sensitivity to movement in the radial direction.
- Stereo formation offers line of sight diversity for wind and surface motion retrieval

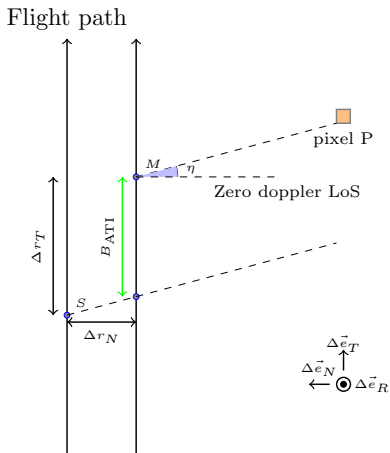
## Relevance

- Coherence time of scattering from the ocean surface  $\mathcal{O}(20 \text{ ms})$  [3]
- $\hookrightarrow$  we typically do not expect a SAR system flying in a formation for cross-track interferometry (XTI) to be able to produce elevation measurements of the surface.
- Due to the too large along-track baseline, the surface becomes decorrelated between observations of the same scene.
- $\hookrightarrow$  The effective along-track baseline must be small enough to allow backscatter from successive looks at the surface to be correlated.

Harmony's bistatic nature, and squinted (off boresight) line of sight, allows for formations where the effective along-track baseline is small enough to make relative elevation measurements of the surface possible.

# Formation Geometry

In a typical SAR the along-track baseline is the physical separation  $\Delta r_T$ . If a squint  $\eta$  is introduced, *the effective along-track baseline is not the physical separation*.  $B_{ATI}$  is a function of the squint angle and the cross-track separation  $\Delta r_N$ .



# Formation Geometry

- Similarly, the effective cross-track baseline is not as in the unsquinted case. Thus, formations can be designed that have small along-track baseline, while maintaining significant cross-track baseline needed for sensitivity to topography.
- The analysis will show that measurements are possible over the swath of Sentinel-1.

# Error in the interferometric measurement

The interferometric phase measured by Harmony will have contributions both from the topography of the scene and from movement in the direction of the line of sight

$$\phi = \phi_{\text{topo}} + \phi_{\text{ATI}} + \phi_n.$$

## Removing the effect of the along-track phase

- The phase due to the along-track baseline  $\phi_{\text{ATI}}$  can be estimated,  $\hat{\phi}_{\text{ATI}}$ , by the two-channel receiver system on-board each of the Harmony satellites.
- The estimate can be subtracted from the measured phase to remove the undesired ATI component.
- The estimator has an error  $\epsilon_{\text{ATI}}$

$$\begin{aligned}\hat{\phi}_{\text{topo}} &= \phi_{\text{topo}} + \epsilon_{\text{ATI}} + \phi_n, \\ \epsilon_{\text{ATI}} &= \phi_{\text{ATI}} - \frac{B_{\parallel}}{B_{\parallel s}} \hat{\phi}_{\text{ATI}},\end{aligned}$$

where  $B_{\parallel}$  is the effective along-track baseline of the two Harmony companions, and  $B_{\parallel s}$  is along-track baseline of the two-channel receiver system.

## Calculating the uncertainty

The Cramer-Rao lower bound for the phase standard deviation [4] is used:

CRLB

$$\sigma_{\phi} = \sqrt{\frac{1 - \gamma^2}{2N_I\gamma^2}},$$

where  $\gamma$  is the coherence and  $N_I$  is the number of independent looks.

# Contributions to the coherence

## Coherence [5]

$$\gamma \approx \gamma_{\text{SNR}} \gamma_t \gamma_{\text{Quant}} \gamma_{\text{Amb}}$$

$\gamma$  is the product of the coherences due to: signal-to-noise ratio  $\gamma_{\text{SNR}}$ , temporal decorrelation  $\gamma_t$ , quantisation  $\gamma_{\text{Quant}}$  and the ambiguities  $\gamma_{\text{Amb}}$ .

The last two contributions are not considered in the analysis as it is expected that SNR and temporal decorrelation will be the dominant contributions to  $\gamma$ .

## SNR and coherence time

### Coherence due to SNR [5]

$$\gamma_{\text{SNR}} = \frac{1}{1 + \text{SNR} (\sigma^0, \text{NESZ})^{-1}},$$

where NESZ stands for the noise-equivalent sigma zero, and  $\sigma^0$  is the backscatter coefficient.

## Coherence time of ocean surface [5] [6] [7]

$$\gamma_t = \gamma_{\text{XTI}}\gamma_{\text{ATI}}, \quad (1)$$

$$\gamma_{\text{XTI}} = 1 - \frac{B_{\perp}}{B_{\perp,c}}, \quad (2)$$

$$\gamma_{\text{ATI}} = e^{-\tau^2/\tau_c^2}, \quad (3)$$

where  $B_{\perp,c}$  is the critical cross-track baseline,  $B_{\perp}$  is the effective cross-track baseline of the Harmony companions,  $\tau = \frac{B_{\parallel}}{2v}$  is the time lag between acquisitions due to the effective along-track baseline and platform velocity  $v$ , and  $\tau_c \approx 3.29\lambda/U$  is the coherence time at wind speed  $U$ .

## Combining the error contributions

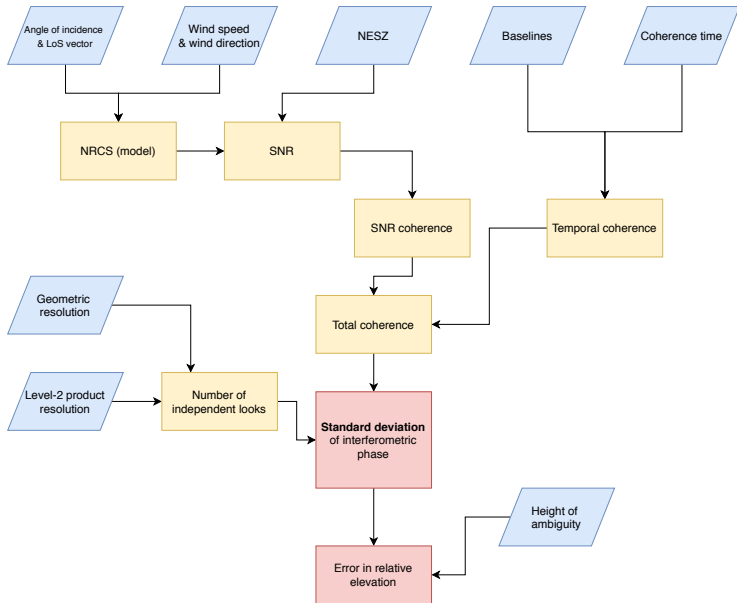
The variance in the measured interferometric phase is the sum of the variance due to the system SNR and temporal decorrelation, and the variance of the estimator  $\hat{\phi}_{\text{ATI}}$

Total Variance

$$\sigma_{\phi} = \sqrt{\sigma_{\phi_n}^2 + \left(\frac{B_{\parallel}}{B_{\parallel s}}\right)^2 \sigma_{\hat{\phi}_{\text{ATI}}}^2},$$

where we have assumed that the two variances are uncorrelated.

# Method of computing the error



# Assumptions in the computation of the performance

- The spatial resolution of the level-2 product strongly affects the error in the result. In the first set of results that we present we have assumed a resolution of  $8 \text{ km} \times 8 \text{ km}$ .
- The SNR of the system is assumed to be 5 dB which is reasonable for SARs [5].

## Formations considered

- The formations are described using the terms  $\alpha\Delta e$  and  $\alpha\Delta\Omega$  [8], where  $\alpha$  is the semi-major axis,  $\Delta e$  is the difference<sup>1</sup>of the the Euclidean norms of the eccentricity vectors, and  $\Delta\Omega$  is the difference of the right ascensions of the ascending nodes of the two companions.
- $\alpha\Delta e$  sets the vertical baseline due to the eccentricity difference and  $\alpha\Delta\Omega$  controls the baseline at the Equator due to the different ascending nodes.

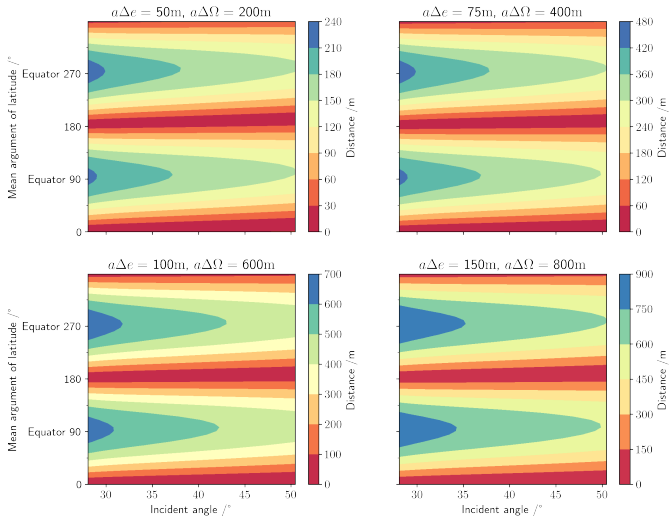
Parameters of the four formations which were used for the performance analysis.

$\alpha\Delta e/m$	$\alpha\Delta\Omega/m$
50	200
75	400
100	600
150	800

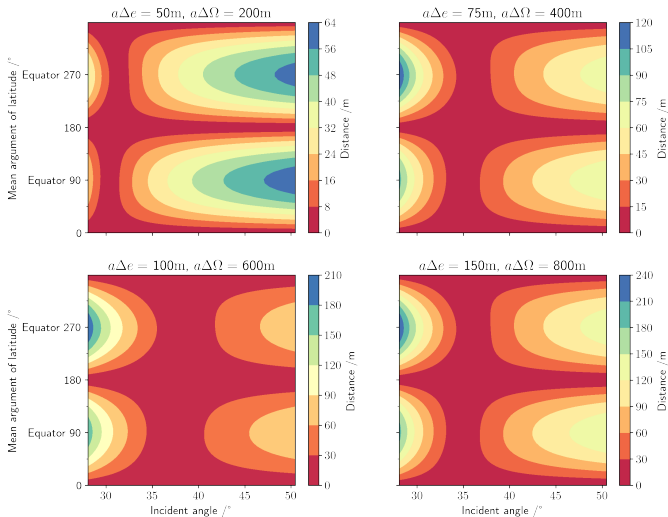
The parameters refer to the formation of the two Harmony companions.

<sup>1</sup> $\Delta$  refers to the difference between the orbits of the two Harmony companions

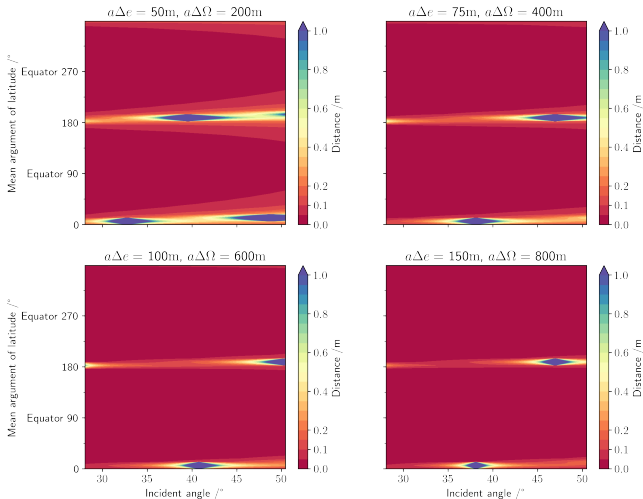
# Cross-track baseline



# Along-track baseline

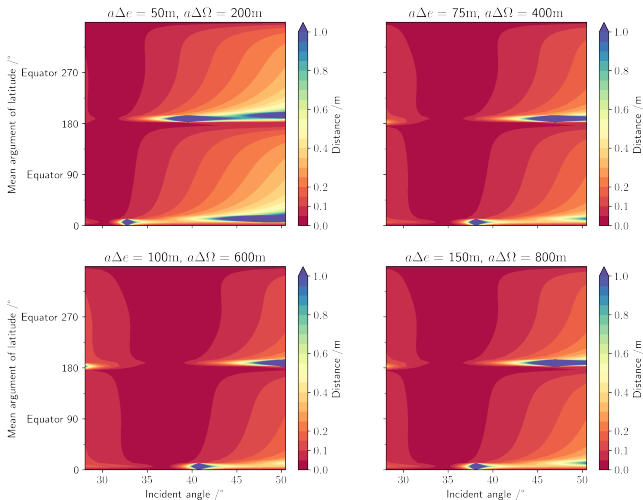


# Uncertainty due to noise



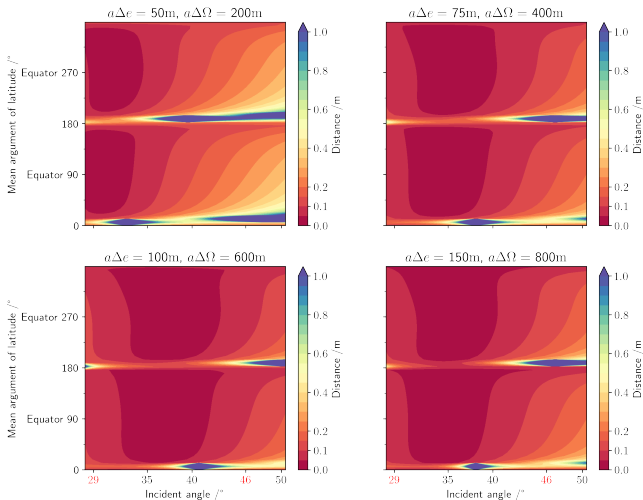
The uncertainty is given in terms of  $1\sigma$ .

# Uncertainty due to ATI phase correction



The uncertainty is given in terms of  $1\sigma$ .

# Total uncertainty



The uncertainty is given in terms of  $1\sigma$ . Note: the limits of S-1 swath in IW swath mode are marked in red on the horizontal axis.

## Discussion

- Results show that the error is  $\mathcal{O}(10 \text{ cm})$  over the majority of the swath, throughout the orbit, with the exception of the poles.
- The range of angles of incidence is wide enough to include the 250 km swath of Sentinel-1.
- Depending on the formation parameters, the height error can be optimised at different points along the swath.
- The performance shown is promising and by increasing the number of independent looks, e.g. setting the product resolution to  $10 \text{ km} \times 10 \text{ km}$ , the performance is enhanced.
- The error rises sharply at the two points during the orbit where the Harmony companions cross each other and their cross-track baseline tends to 0 m.

## Sea-state bias

- The sea state bias is a source of error that was not considered in the analysis.
- We expect the sea-state bias to be a function of wind speed, wave height and incidence angle.
- Sea-state bias models can likely be estimated using comparable methods as for SWOT.
- The correction uncertainty is expected to be in the order of cm.

## The way forward

- Constrained optimisation of the formation parameters to reduce the error should be performed.
- The variation of the SNR over the swath will be included in the analysis, by incorporating models for the ocean backscattering.
- The antenna pattern of typical SAR systems will be accounted for in the analysis to calculate how the NESZ varies with different polarisations.
- Estimate the impact of sea-state bias on the performance.

# References I

- [1] P. Lopez Dekker, B. Chapron, P. Prats, et al. "STEREOID: a Sentinel-1 companion mission to observe land, ice, and ocean surface dynamics". In: Presented at the Living Planet Symposium, Milan, Italy, 2019.
- [2] M. Kleinherenbrink, A. Theodosiou, Y. Li, et al. "Harmony: measuring instantaneous sea-ice dynamics from space". en. In: *The Cryosphere* (2020). To be submitted.
- [3] R. D. Chapman, B. L. Gotwols, and R. E. Sterner II. "On the statistics of the phase of microwave backscatter from the ocean surface". In: *Journal of Geophysical Research: Oceans* 99.C8 (1994), pp. 16293–16301. DOI: 10.1029/94JC01111.
- [4] M.S. Seymour and I.G. Cumming. "Maximum likelihood estimation for SAR interferometry". In: *Proceedings of IGARSS '94 - 1994 IEEE International Geoscience and Remote Sensing Symposium*. Vol. 4. Aug. 1994, 2272–2275 vol.4. DOI: 10.1109/IGARSS.1994.399711.

## References II

- [5] Steffen Wollstadt, Paco López-Dekker, Francesco De Zan, et al. “Design Principles and Considerations for Spaceborne ATI SAR-Based Observations of Ocean Surface Velocity Vectors”. In: *IEEE Transactions on Geoscience and Remote Sensing* 55.8 (Aug. 2017), pp. 4500–4519. ISSN: 1558-0644. DOI: 10.1109/TGRS.2017.2692880.
- [6] H.A. Zebker and J. Villasenor. “Decorrelation in interferometric radar echoes”. In: *IEEE Transactions on Geoscience and Remote Sensing* 30.5 (Sept. 1992), pp. 950–959. ISSN: 1558-0644. DOI: 10.1109/36.175330.
- [7] S.J. Frasier and A.J. Camps. “Dual-beam interferometry for ocean surface current vector mapping”. In: *IEEE Transactions on Geoscience and Remote Sensing* 39.2 (Feb. 2001), pp. 401–414. ISSN: 1558-0644. DOI: 10.1109/36.905248.
- [8] Simone D’Amico and Oliver Montenbruck. “Proximity Operations of Formation-Flying Spacecraft Using an Eccentricity/Inclination Vector Separation”. en. In: *Journal of Guidance, Control, and Dynamics* 29.3 (May 2006). Number: 3 Reporter: Journal of Guidance, Control, and Dynamics, pp. 554–563. ISSN: 0731-5090, 1533-3884. DOI: 10.2514/1.15114. URL: <http://arc.aiaa.org/doi/10.2514/1.15114> (visited on 10/11/2019).